J Neurophysiol 104: 2543–2555, 2010.
First published July 14, 2010; doi:10.1152/jn.00256.2010.

Neural Heterogeneity and Efficient Population Codes for Communication Signals

Gary Marsat and Leonard Maler
Department of Cellular and Molecular Medicine, University of Ottawa, Ottawa, Canada

Submitted 11 March 2010; accepted in final form 8 July 2010

Marsat G, Maler L. Neural heterogeneity and efficient population codes for communication signals. *J Neurophysiol* 104: 2543–2555, 2010. First published July 14, 2010; doi:10.1152/jn.00256.2010. Efficient sensory coding implies that populations of neurons should represent information-rich aspects of a signal with little redundancy-.Recent studies have shown that neural heterogeneity in higher brain areas enhances the efficiency of encoding by reducing redundancy across the population. Here, we study how neural heterogeneity in the early stages of sensory processing influences the efficiency of population codes. Through the analysis of in vivo recordings, we contrast the encoding of two types of communication signals of electric fishes in the most peripheral sensory area of the CNS, the electrosensory lateral line lobe (ELL). We show that communication signals used during courtship (big chirps) and during aggressive encounters (small chirps) are encoded by different populations of ELL pyramidal cells, namely I-cells and E-cells, respectively. Most importantly, we show that the encoding strategy differs for the two signals and we argue that these differences allow these cell types to encode specifically information-rich features of the signals. Small chirps are detected, and their timing is accurately signaled through stereotyped spike bursts, whereas the shape of big chirps is accurately represented by variable increases in firing rate. Furthermore, we show that the heterogeneity across I-cells enhances the efficiency of the population code and thus permits the accurate discrimination of different quality courtship signals. Our study shows the importance of neural heterogeneity early in a sensory system and that it initiates the sparsification of sensory representation thereby contributing to the efficiency of the neural code.

INTRODUCTION

The nervous system must acquire sensory information from its ,environment and a central theme in neuroscience to determine how this is done efficiently. The ideas of Barlow (1961) on efficient neural encoding of sensory signals have long guided both experimental and theoretical studies of sensory processing. Efficient neural coding implies that sensory neurons must reliably encode behaviorally relevant and information-rich aspects of sensory signals. Furthermore, the pattern of encoding spikes and their segregation into different neuronal streams must permit rapid signal classification and discrimination by downstream neural networks. Communication signals, with their remarkable diversity and ability to convey many types of information, are arguably the best examples to which these principles should be applied. Some communication signals are discrete and simply act to identify the presence of a conspecific or their sex (Miller et al. 2003). Other signals, such as those related to courtship, are graded and permit females to judge the relative fitness of their suitors (Andersson 1994; Zahavi 1975). According to Barlow's principles, different neural streams and codes should be involved in the processing of these different signal classes. To test this hypothesis, we compare, in the first part of this paper, the encoding of two types of communication signals in the electric fish *Apteronotus leptorhynchus*: one is a signal that occurs primarily during male–male agonistic interactions, whereas the second is associated with courtship (Bastian et al. 2001; Hagedorn and Heiligenberg 1985; Hopkins 1972). In the second part of the paper, we focus on the courtship signal to show how neural heterogeneity enhances the encoding of the quality of the courtship signals.

A. leptorhynchus has a constant sinusoidal electric organ discharge (EOD; females: ~600–800 Hz, males: >800 Hz). The EOD drives, in a probabilistic manner, the baseline discharge of electroreceptors (P-units) distributed over the body (Nelson et al. 1997); P-units code for all electrosensory input (navigation, prey detection, and communication) and can therefore be considered to convey a dense population code. The proximity of a conspecific results in an AM of the EOD—or beat—and the beat frequency conveys the sex of the fish (Hagedorn and Heiligenberg 1985; Zakon and Dunlap 1999). The most common communication signals produced—chirps—consist of brief increases in EOD frequency (Engler et al. 2000; Hupé and Lewis 2008). Low-frequency beats (same sex interactions) trigger the production of small chirps (~100 Hz frequency increase) that are believed to deter male aggressive behavior (Hupé and Lewis 2008). Small chirps are encoded by an increase in the firing rate and synchronization of P-units (Benda et al. 2005, 2006). In contrast, high-frequency beats (different sexes interactions) trigger big chirps (in males; ~300–900 Hz frequency increases), which are commonly observed in courtship settings (Bastian et al. 2001; Hagedorn and Heiligenberg 1985; Hopkins 1972). They can take on a wide range of sizes and shapes (Bastian et al. 2001; Dunlap and Larkins-Ford 2003; Zupanc and Maler 1993). High-frequency beats evoke a synchronized discharge of the P-unit population, and big chirps cause their desynchronization without any change in mean firing rate (Benda et al. 2006).

P-units, in turn, project to the pyramidal cells of the medullary electrosensory lateral line lobe (ELL). The ELL is organized into three topographic electrosensory maps, and the pyramidal cells within each map are further organized into columns (Maler 2009a,b). Pyramidal cells exhibit remarkable cellular/molecular and physiological diversity across both maps and columns within each map (Maler 2009a,b). The first and major source of functional diversity is the morphological subdivision of pyramidal cells into E (basilar) and I (nonbasilar) types (Maler 1979; Saunders and Bastian 1984). E-cells

Address for reprint requests and other correspondence: G. Marsat, 451 Smyth Rd., Ottawa, ON, Canada K1H8M5.

respond with firing rate increases to increases in EOD intensity within their receptive fields. I-cells are inhibited by increases in EOD intensity and instead increase their firing rate to decreases of EOD intensity within their receptive field. We show below that the E- versus I-cell dichotomy is essential to the immediate differential neural encoding of small versus large chirps. We go on to show that the cellular heterogeneity within the I-cell class is likely responsible for a diversity in responsiveness to large chirps.

We first show that the diversity of ELL pyramidal cell types is immediately responsible for an initial sparsification of the P-unit population code. We have previously shown that small chirps evoke synchronized and stereotyped spike bursts in a subset of target pyramidal cells (E-cells) of the ELL (Marsat et al. 2009). In contrast, we will show here that big chirps are encoded by a completely disjunct population: I type pyramidal cells. We propose that this initial sparsification allows for efficient downstream decoding of both chirp types. Furthermore, we will argue that the different neural codes used for their representation reflect the difference in structure between chirp types. Small chirps are discrete signals whose rate of production varies as a function of the agonistic state of a male (Dulka and Maler 1994; Hupé and Lewis 2008); we show below that, although small chirps can be readily detected by E-cells, different small chirps cannot be discriminated from one another. In contrast, big chirps are produced at lower rates but have a wider range of shapes and durations (Bastian et al. 2001). The structure of these chirps is influenced by the hormonal state of the male (Dulka et al. 1995) and thus presumably its readiness to spawn. If big chirps carry information about the fitness of the male or its readiness to spawn, the female's electrosensory system should be able to encode their detailed temporal structure to discriminate between big chirps of different quality.

It has been shown that the spike trains of single neurons can carry the information necessary to discriminate between small variations of a given communication signal (Machens et al. 2003; Narayan et al. 2007; Ronacher et al. 2008). It is unknown, however, how the responses from a population of neurons might combine to encode subtle differences across a class of communication signals. Pooling the responses across a population of neurons can improve stimulus estimation and discrimination for at least two reasons: either because the neurons encode the signal differently, thereby providing complementary descriptions of the stimulus (Bell and Sejnowski 1995; Chechik et al. 2006; Osborne et al. 2008), and/or because the noise in the responses is partially—or completel—uncorrelated, thereby allowing it to be averaged out from the population response (Aertsen et al. 1989; Chelaru and Dragoi 2008; Shamir and Sompolinsky 2006). Moreover, several of these studies point out that the heterogeneity of response properties enhances the efficiency of the population code. The importance of heterogeneity has been shown theoretically and experimentally in brain areas remote from the periphery (e.g., cortex: Chelaru and Dragoi 2008; Osborne et al. 2008; inferior colliculus: Holmstrom et al. 2010). Sparse representation of sensory signals in higher brain areas involves a nonredundant encoding of the signal by heterogeneous population of cells; but it is unclear how this sparsification is initiated close to the periphery and what role neural heterogeneity plays in this process. In this study, we draw a link between the heterogeneity at the lowest level of the CNS of electric fish—the ELL—and the efficient encoding of communication signals. Specifically we show that two type of heterogeneity participate in a sparsification of the representation of the signal: a coarse heterogeneity (E-cells vs. I-cells) that underlies the differentiation of different type of signals and a more subtle heterogeneity (within I-cells) that improves discrimination of signals within one signal type (courtship chirps).

METHODS

Electrophysiology

Surgery was as previously described (Marsat et al. 2009; Middleton et al. 2006). Briefly, *A. leptorhynchus* were anesthetized with tricaine methanesulfonate (Finquel MS222, Argent Chemical Laboratories, Redmond, WA) and respirated during surgery. The skull above the ELL was removed after local anesthetic was applied to the wound. The skull was glued to a post for stability. General anesthesia was stopped, and the fish was immobilized with an injection of curare (pancuronium bromide, Holzkirchen, Germany) and transferred to the experimental tank ($40 \times 45 \times 20$ cm) containing water kept between 25 and 27°C and with conductivity around 100–400 μS. In vivo, single-unit recordings were performed using metal-filled extracellular electrodes (Frank and Becker 1964). Pyramidal cells can easily be located by the anatomy of the ELL and overlying cerebellum as well as by their response properties (Maler et al. 1991; Saunders and Bastian 1984). Medio-lateral recording position and depth of penetration (in the dorsal-ventral plane) was monitored and used to estimate electrode placement relative to the three maps of the ELL. Except where otherwise noted, recordings are from the lateral segment. All experiments and protocols were approved by the University of Ottawa Animal Care Committee.

Stimulation

The unperturbed EOD was recorded between the head and the tail of the fish. Each EOD cycle triggered a sine wave generator (195 Universal waveform generator, Fluke, Everett, WA) to output one cycle of a sinusoidal signal of frequency matching that of the fish's EOD. This sinusoidal output was modulated by multiplication with our AM signal. AM signals were created off-line with a sampling rate of 10 kHz. Stimuli were attenuated (PA4, Tucker-Davis Technologies, Alachua, FL), isolated (model 2200, A-M Systems, Carlsborg, WA), and delivered through two stimulation electrodes placed on either side of the fish, parallel to its longitudinal axis; this arrangement mimics the stimulus geometry of electrocommunication signals (Kelly et al. 2008) and is referred to as global stimulation because electroreceptors over the entire body surface are stimulated. Local stimulation was delivered through a dipole centered on the cell's receptive field. After locating the cell's receptive field by finding the position of a local stimulation dipole that best excites the cell, an additional dipole was used to measure the amplitude of the stimulus near the cell's receptive field. Recordings of the cells were used for analysis only if the neuron produced a clear response to locally presented (within the neurons receptive field center) sinusoidal stimuli. For both local and global geometries, stimulus intensity was adjusted to obtain a difference of the amplitudes of the EOD between the top and the bottom of a beat cycle corresponding to 15–20% the baseline EOD amplitude. Therefore for each cell, the local and global stimulus intensity was approximately equal within the cells receptive field.

The stimulus envelope of chirp stimuli consisted of a sinusoidal modulation (the beat, 120 Hz for big chirps, and 5 Hz for small chirps) punctuated every second by a chirp. Chirp shape was calculated, as published previously (Benda et al. 2005, 2006), assuming a Gaussian frequency increase in the EOD during chirping. The duration of big

chirps (at 10% height) was either 15, 30, or 45 ms and was 14 ms for small chirps. The increases in frequency of the EOD during the chirps were chosen to cover the whole range of frequencies occurring naturally (Bastian et al. 2001; Supplementary Fig. S1)[1]: 300, 600, or 900 Hz for big chirps and 60, 100, or 122 Hz for small chirps.1 The increase in frequency during a big chirp is accompanied with—and linearly correlated to (Turner et al. 2007; Supplementary Fig. S1)—a decrease in the amplitude of the EOD, so we co-varied these two factors when making the artificial big chirp stimuli. Based on Supplementary Fig. S1, we chose three amplitude decreases (−25, −50, and −75%), corresponding to the frequency increases of 300, 600, and 900 Hz, respectively, and that also covered the range of amplitude decreases observed. In this study, we mostly refer to the combined frequency-AM by its amplitude. The phase at which small chirps occurred relative to the beat was either the minimum of the trough or midway in the rising phase (see Fig. 4*A*).

Randomly amplitude modulated stimuli (RAM) were designed to replicate the characteristics of big chirps and thus consisted of a beat AM (200 Hz) and a random envelope modulation (0–60 Hz). This envelope modulation corresponds to the envelope associated with big chirps (see RESULTS) that is encoded in the neural response. The envelope was produced by low-pass filtering Gaussian white noise. The filter cut-off (60 Hz) was chosen to encompass the frequencies typically present in big chirps (Supplementary Fig. S2).

Detection analysis

Detection analysis relies on comparing the number of spikes elicited by chirps and by the beat in small time windows of length L (10, 20, or 50 ms) of the binarized spike trains (Supplementary Fig. S3). For each chirp, only the window (starting within 50 ms of chirp beginning) with the most spikes was used to quantify the maximum spike rate for that chirp. Windows with the most spikes during each beat cycle of small chirp stimuli were used for further analysis. For big chirp stimuli, windows with the most spikes in the 600 ms preceding each big chirp were used. Maximum firing rates of individual responses $B(t)$, or population responses $PB(t)$ of N neurons (i.e., the sum of N individual responses), were calculated as $F = 1/N \times L \sum_{t=0}^{L} [PB(t)]$. The probability distributions of maximum firing rates during chirps $P(F_{chirp})$ and during the beat $P(F_{beat})$ were used to calculate the percentage of error made by an ideal observer trying to discriminate chirps from the background beat—in other words, trying to detect chirps—based on the number of spikes elicited. Receiver operating characteristic curves were generated by varying a threshold firing rate T. For each threshold value, the probability of detection (P_D) was calculated as the sum of $P(F_{chirp} > T)$, and the probability of false alarm (P_F) as the sum of $P(F_{beat} > T)$. The error level for each threshold value is $E = 1/2P_F + 1/2(1 - P_D)$. The detection error levels reported in the figures are the minimum values of E.

Discrimination analysis

Our analysis is based on the van Rossum (2001) method of quantifying spike train similarity (see also Supplementary Fig. S3). Each spike train $B(t)$, expressed as a binary sequence, was convolved with a filter resulting in $R(t)$. In the analysis using shuffled spike trains, the timing of each spike (within the chirp response) was randomly changed before convolving the spike trains with the filter. The filter used was an α function of the form $f(t) = t[\exp(-2.45t/\tau)]$, where τ is the width of the function at half-maximum (Machens et al. 2003). The original technique (van Rossum 2001) used an exponential function for this step. We repeated our analysis with an exponential of the form $f(t) = \exp(-t/\tau)$, but the results were very similar; therefore we display the results calculated using the α function because it is a biologically more relevant shape. A small portion of the recording surrounding the chirps was extracted for further processing (−15 to 30 ms relative to the middle of big chirps and −10 to 30 ms relative to small chirps). The distance D_{xy} between the two spike trains x and y of length L is defined as $D_{xy} = 1/L \sum_{t=0}^{L} [R_z(t) - R_y(t)]^2$.

Previous uses of this method were restricted to the comparison of two spike trains. Here we used a simple method of applying this measure to multiple spike trains—we combined n spike trains by averaging them: $PR(t) = \sum_{i=t}^{n} [R_i(t)]/n$. The resulting variable $PR(t)$ represents a population response and can be seen as mimicking the postsynaptic potential of a cell integrating several inputs $[R_i(t)]$ with similar weights.

The different spike trains in the combination were selected randomly from our pool of recordings and came either from the same cell, mimicking a homogenous population of cells, or from different cells, thus taking in account cell heterogeneity in the analysis. For each comparison, we tried to use all possible combinations of spike trains but had to limit it to 200 randomly selected combinations when the number of possibilities was too large given the number of spike trains available and the number included in the combination.

For a given comparison between the responses to chirps X and Y, the distance D_{xy} was calculated for all possible pairs of combined response $PR_x(t)$ and $PR_y(t)$, creating a large array of distances D_{XY}. We also calculated the distance D_{XX} and D_{YY} between pairs of responses to the same chirp. The average of D_{XX} and D_{YY} is used for the next step of the analysis and denoted as D_{XX} for simplicity . For the analysis of small chirps, a given chirp presented at different phases of the beat is either considered a different stimulus(to assess discriminability of AM shapes) or the same stimulus (to assess discriminability of chirps). For the discrimination analysis relying on response correlation rather than response distance (Fig. 7), the correlation coefficient between the responses was used instead of the distance measure; the rest of the procedure is identical.

The probability distributions $P(D_{XY})$ and $P(D_{XX})$ of values in the arrays D_{XY} and D_{XX} were used to determine the proportion of errors made by an ideal observer trying to discriminate between the two distributions. Receiver operating characteristic curves were generated by varying a threshold distance level T. For each threshold value, the probability of detection (P_D) is calculated as the sum of $P(D_{XY} > T)$, and the probability of false alarm (P_F) as the sum of $P(D_{XX} > T)$. The error level for each threshold value is $E = 1/2P_F + 1/2(1 - P_D)$. The discrimination error levels reported in the figures are the minimum values of E.

Information theoretic analysis

Envelope signals were extracted via a Hilbert transform from the local recording of the EOD amplitude rather than using the original envelope used to produce the stimulus. This precaution ensures that the signal used in the analysis is the one actually stimulating the cells and that the analysis is not sensitive to small distortions caused, for example, by a low sampling of the envelope signal by the underlying 200 Hz beat.

We discarded the first second of stimulation during which firing rate might adapt. Spike trains where expressed as binary sequences sampled at 2,000 Hz. The first-order kernels describe the linear relationship between the stimulus and the neuron's firing rate (Clague et al. 1997; Theunissen et al. 1996). Arrays representing the firing rate, $r(t)$ and stimulus envelope, $s(t)$, were expressed as variations around their respective means, yielding $r'(t)$ and $s'(t)$. These arrays were segmented and Fourier-transformed, yielding $R'(f)$ and $S'(f)$. The frequency-domain representation of the linear kernel for response i was calculated as: $H_i(t) = \langle R_i(f) * S(f) \rangle / \langle R_i(f) R_i(f) * \rangle$. $H_i(f)$ was converted to the time domain, $h_i(t)$, using the inverse Fourier transform. The result of these operations is equivalent to the cross-correlation of $r'_i(t)$ and $s'(t)$, divided by the autocorrelation of $r'_i(t)$ (Press et al. 1992).

[1] The online version of this article contains supplemental data.

$h_i(t)$ was averaged across several responses of the same cells (typically 4–5) to give the average kernels $h(t)$ shown in Fig. 8.

Information transfer functions were calculated by convolving $h(t)$ with $r_i(t)$ to reconstruct the neuron's estimate of the stimulus, $est_i(t)$. To mimic a homogeneous population, we convolved $r_i(t)$ with the mean kernel across cells. To produce stimulus estimates from population responses, $est_j(t)$, the estimates from several responses were averaged. Noise, $n_j(t)$, was computed as $s(t) - est_j(t)$. Signal-to-noise ratio, $SNR_j(f)$, was computed as the power spectrum of $est_j(t)$ divided by that of $n_j(t)$. $SNR_j(f)$ was averaged across many combinations of responses, and information transfer functions were calculated from $SNR(f)$ as $I(f) = \log_2[1 + SNR(f)]$ (Borst and Theunissen 1999). All data analysis was performed using Matlab 2008b (Mathworks, Natick, MA).

RESULTS

Both small and large chirps are detected

In vivo recordings of pyramidal cells of the ELL were performed to characterize their response to a variety of small and big chirps. The structures of small chirp and big chirp stimuli are shown in Fig. 1. In subsequent figures, we represent the chirp stimuli by their associated AMs.

The ELL is divided into three maps [centromedial (CMS), centrolateral (CLS), and lateral (LS)], each receiving a topographic map of electroreceptors (Carr et al. 1982; Heiligenberg and Dye 1982). Pyramidal cells within each map are first divided into two major classes: E-type cells whose firing rate increases in response to increases in EOD amplitude and I-type cells whose firing rate increases in response to decreases in EOD amplitude (Maler 1979; Saunders and Bastian 1984). E- and I-type cells are further subdivided into superficial, intermediate, and deep varieties based on a large number of morphological, physiological, and molecular criteria (Bastian and Nguyenkim 2001; Maler 2009a).

Big chirps occur in the context of a high-frequency beat that evokes strongly synchronized firing of P-units (Benda et al. 2006). Most I-cells respond poorly or not at all to the high-frequency beat, consistent with the low-frequency tuning of this cell class in all three ELL maps seen both in vivo (Krahe et al. 2008) and in vitro (Mehaffey et al. 2008). Big chirps induce a desynchronization of the P-unit population without a change in their mean firing rate (Benda et al. 2006); remarkably, this desynchronization is sufficient to elicit a small increase in the firing rate of I-cells (Fig. 1*A*). All types of I-cells respond to big chirps (superficial, intermediate, and deep; Supplementary Fig. S4), thereby increasing the diversity of I-cells responding to these signals. I cells from all three maps respond similarly to big chirps (Supplementary Fig. S4).The analysis below concentrates on cells of the LS, but the results are qualitatively similar if responses of I-cells from CMS and CLS are included in the analysis (data not shown). In addition to P-units, a variety of other inputs influence the response properties of pyramidal cells, and one way to reveal their importance is to compare the responses to stimuli presented locally and globally. Communication stimuli are global signals that affect the whole surface of the skin. The same stimuli can be presented locally in the receptive field of the cell. Although both local and global stimuli drive the electroreceptors connected to the pyramidal cell in a similar manner, global stimuli also drive additional network inputs to the cell (e.g., feedback; ovoid cells; gap junction inputs from interneurons; Berman and Maler 1999). The response to big chirps is greatly reduced if the global network inputs are not stimulated (Fig. 2), suggesting that some of these nonlocal inputs are essential for generating the evoked big chirp response in I-cells. This conclusion is consistent with our previous demonstration that the E-cell response to small chirps required global network inputs (Marsat et al. 2009). E-cells ceased to discharge for the duration of big chirps (Supplementary Fig. S5). Again it is interesting to note that this cessation of E-cell spiking is caused by the big chirp–induced desynchronization of P-unit input and not the mean P-unit firing rate, which is unchanged by a big chirp (Benda et al. 2006).

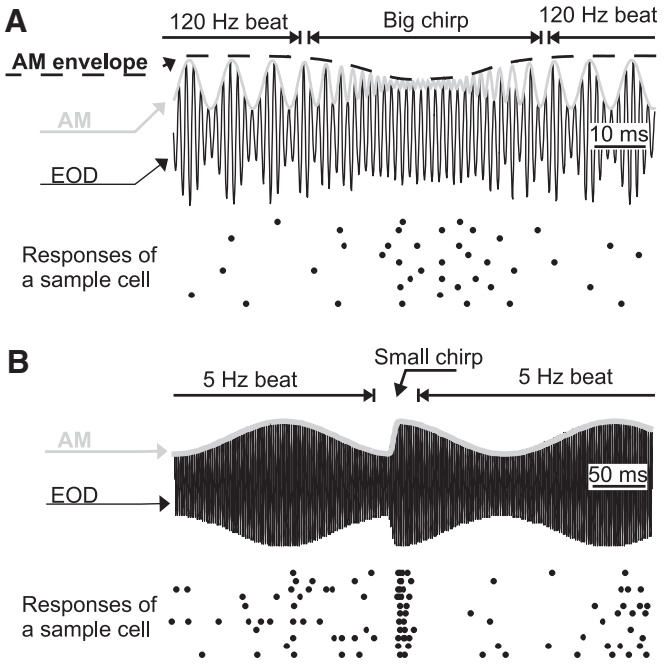

FIG. 1. Big and small chirps and the response they elicit in the electrosensory lateral line lobe (ELL). *A*: big chirps. The electric organ discharge (EOD; thin black line) of the fish is modulated in amplitude (gray line) in the presence of another fish. The ongoing sinusoidal modulation (beat) is interrupted by chirps. Big chirps result in an increase in beat frequency and decrease in amplitude. This decrease in amplitude causes a modulation in the envelope of the AM (i.e., 2nd-order envelope, dashed line). The strength of the stimulus is large in this diagram for purposes of clarity, but it is normally adjusted so that the regular beat causes a modulation depth of ~20% of the unperturbed EOD. The raster plot shows the responses of a representative I cell. *B*: small chirps. The stimulus is shown in a similar fashion as that in *A,* and the responses of an E-cell are displayed. Small chirps, like big chirps, consist of a transient increase in the AM frequency. However, unlike big chirps, they are not accompanied by a significant amplitude decrease. Also, because small chirps are studied here in the context of male–male interactions, they are associated with low-frequency beats. For this reason, these stimuli do not have an AM envelope (2nd-order envelope). Note the 5× difference in time scale between *A* and *B*.

Small chirps are encoded by a stereotyped burst response in E-cells synchronized to chirp onset (Fig. 1*B*) (Marsat et al. 2009). Our previous results (Marsat et al. 2009) showed that a strong burst response is confined to the superficial E-cells of the LS. Intermediate and deep E-cells (LS) and all cells in CMS/CLS fired with similar strength during the beat and the chirp. This result is consistent with earlier work (Metzner and Juranek 1997), showing that LS is most involved in processing communication signals. Furthermore, I-cells of all segments and layers responded with similar firing rates during beat and

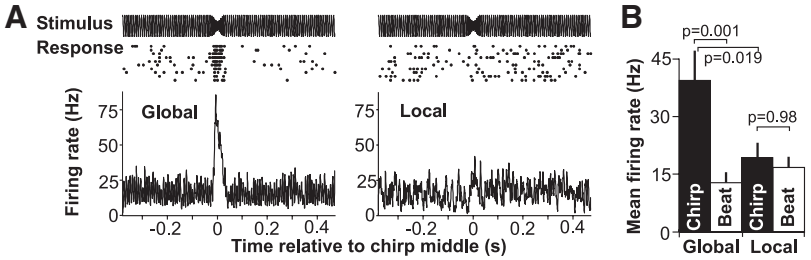

FIG. 2. Chirp response requires global network inputs. *A*: examples of the response to 1 chirp when the stimulus is presented globally to the whole skin surface (thus recruiting most electroreceptors and the entire ELL + feedback network) or locally to the cell's receptive field (stimulating only the receptors of the classical receptive field). We show raster plots of the response of 1 cell and the mean firing rate across cells ($n = 19$ cells). *B*: mean firing rate in response to global and local chirps and beat. We used a 200 ms portion of the beat response preceding each chirps and compared it with the chirp response starting 15 ms before the middle of the chirp and ending 30 ms after. For each portion of response, the ratio (number of spikes/window duration) was averaged across repetitions for each cell. The average (±SE, $n = 19$) across cells is shown with *P* values of ANOVA followed by Tukey test.

chirps (Marsat et al. 2009), making small chirps difficult and perhaps impossible to detect based uniquely on I-cell responses.

Reliable detection of the occurrence of a chirp (small or big) could occur readily if the number of evoked spikes was significantly different from the number of spikes elicited by the background beat. To assess the reliability of chirp detection, we quantified the number of spikes triggered by beat and chirp stimuli over different time windows. Our analysis shows that combining the responses from three cells would not be sufficient to reliably have more spikes during the chirps than during the beat (Fig. 3). This is shown by the fact that the spike counts in a 10 ms window during the beat overlap with the spike counts during the chirps (i.e., the distributions overlap in Fig. 3*A, left*). When chirp detection relies on the summed spike count or mean firing rate (over a narrow time window) of 10 cells, however, the reliable difference could lead to accurate chirp detection of both small and big chirps (i.e., the distributions do not overlap in Fig. 3*A, right*). An ideal decoder, such as a target cells in the midbrain [torus semicircularis (TS)] (Maler 2007), receiving the output from a population of ELL cells, could detect the occurrence of respectively small and big chirps reliably only if the distribution of spike counts during the beat and during the chirps have little overlap. For example, assuming an ideal threshold of 100 Hz, a decoder receiving inputs from 10 superficial E-cells (LS) would always respond to small chirps but never to the beat because the beat does not elicit mean firing rates above 100 Hz, and small chirps do not elicit mean firing rates below 100 Hz. Note that for small chirps, this ideal threshold is around 100 Hz, reflecting the bursting nature of the E-cell chirp response (i.e., >1 spike per 10 ms window; see also Marsat et al. 2009). Big chirps typically do not trigger bursts and, for TS cells receiving 10 I-cell inputs, an ideal threshold of ~67 Hz would optimally separate the beat and big chirp responses.

Based on this principle, the TS decoders would classify the response as being elicited by small/big chirps if the mean firing rate of the E/I-cell population input was above the optimal threshold. Any overlap between the distributions of firing rates during the chirp and during the beat would lead to incorrect classification. We show in Fig. 3*B* the percentage of errors of such a decoder as a function of the number of cells included in the population response. We varied the time window over which the mean firing rate of the population was evaluated. Our result shows that in most cases the decoder would accurately detect either the small or big chirp by pooling the responses from 10 cells (E or I, respectively). Note that the response to small chirps was typically very brief (~15 ms; see also Marsat et al. 2009)

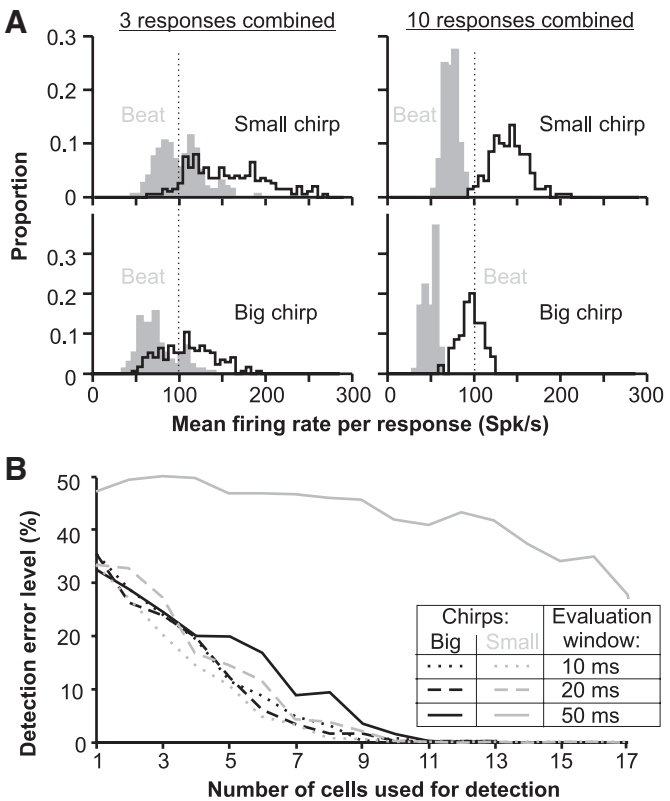

FIG. 3. Detection of big and small chirps by pyramidal cells. *A*: firing rates of I-cells after big chirps and of E-cells after small chirps. Only the responses of superficial E-cells of the lateral (LS) were used. Individual responses from several cells were combined. For each chirp or beat cycle, we selected the 10 ms window that contained the most spikes in the combined responses and display the distribution of mean firing rates per response during these windows. Dashed lines indicate the theoretical limit of burst firing rates (>1 spike per 10 ms) of a single neuron based on modeling studies (Turner et al. 2002). *B*: detection performance as a function of the number of responses combined. Histograms such as the ones shown in *A* are used to assess the degree of separation between the 2 distributions. Any overlap between the 2 distributions leads to errors in detection; total overlap would lead to chance performance (50% error). Detection performance was quantified by calculating the mean number of spikes per response over a 10, 20, or 50 ms window.

and thus averaging the firing rate over 50 ms would lead to poor detection accuracy (Fig. 3*B*, solid gray line).

Chirp discrimination: the structure of small chirps prevents their discrimination

The previous section showed that the presence of a chirp (small or big) can be accurately detected by the population of pyramidal cells (E or I). We do not know, however, if the information carried by quantitative variation in the duration and/or size of chirps can be extracted from the population response. Electric fish produce chirps of a variety of durations (big chirps: 10 to >50 ms; small chirps: 10 to ~20 ms) and sizes (big chirps: 250 to >900 Hz; small chirps: 40 to 150 Hz). Two differences between small and big chirps have a crucial impact on their shapes: *1*) for big chirps, but not for small chirps, the increase in frequency is accompanied by a decrease in the amplitude of the EOD; and *2*) small chirps are delivered on a low frequency beat, and the shape of the resulting AM will be determined by the phase of the beat at which they occur as much as by the duration or magnitude of the chirp (Zupanc and Maler 1993). Because big chirps are much longer than the period of the beat on which they are superimposed, the shape of the AM is essentially independent of its phase relationship with the beat. The importance of this last factor has to be stressed because it is crucial to the understanding of how these communication signals are encoded. The characteristics of a big chirp, its size and length, will be reflected in the size and length of the amplitude modulations of the stimulus. A small chirp of a given size and length can occur at any phase of the beat; there is no systematic relationship between chirp timing and beat phase (Zupanc and Maler 1993). As a consequence, the same small chirps will produce different amplitude modulations depending on where it occurs during the beat. In other words, the fish might be able to control the duration and size of small chirps it produces, but it will not determine the shape of the AMs received by neighboring fish. This effect is shown in Fig. 4*A*, where two similar AMs are caused by different small chirps, whereas the same chirp causes two different AMs when it occurs at different phases.

These three different small chirp AMs all cause a highly stereotyped burst response in the pyramidal cells (E-cells; Fig. 4*A*). The details of the burst structure seem to vary slightly from chirp to chirp; for example, the left-most response in Fig. 4*A* has more spikes. Therefore we first determined whether the responses of these cells could allow an ideal observer to discriminate between AMs of different shapes. In this first analysis, the phase at which the different chirps occur is kept fixed, and we assessed the discriminability of these fixed phase chirps. This task amounts to discriminating signals with different AM shapes.

Instead of using a decoder that simply compares the number of spikes elicited by the two stimuli (here two chirps), as we did above, our decoder also takes in account the structure of the spike trains (see METHODS and Supplementary Fig. S3). To do so, the responses are represented as time-dependent firing rates rather that average firing rates. The differences between responses are assessed by a commonly used measure of spike train distance (van Rossum 2001). The gray line in Fig. 4*B* shows that the population response will allow the decoder to discriminate fixed-phase small chirps in 90% of the cases when

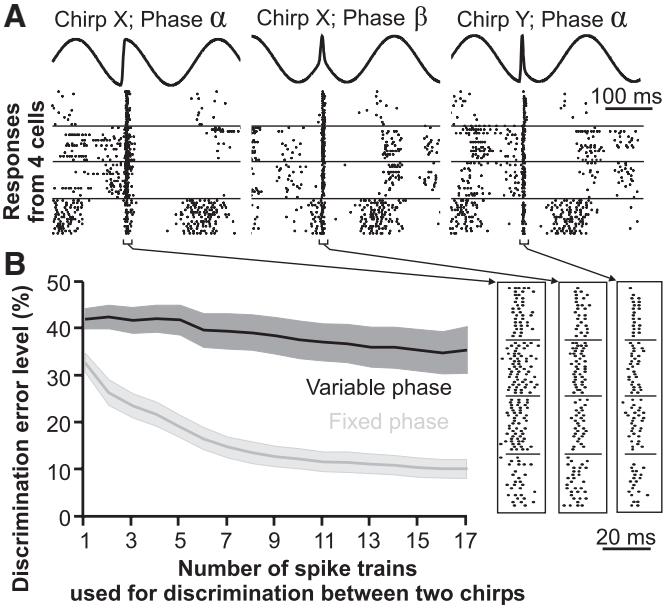

FIG. 4. Small chirps cannot be discriminated by pyramidal cells. *A*: examples of small chirps and the responses of an E pyramidal cell. The shape of the AM caused by a chirp is influenced by the characteristics of the chirp (size, duration) but also by the phase at which it occurs. We show 3 stimuli that correspond either to a difference in chirp characteristics (chirp X vs. chirp Y) or a difference in the phase at which it occurs (phase α or β). Below the stimuli we show raster plots of the responses of 4 cells with an *inset* showing the detailed structure of the responses. *B*: mean discriminability ($\pm$SE; $n = 15$ chirp pairs for the gray line and 3 for the black line) of small chirps by E-cells. Our analysis quantifies the discriminability of chirp pairs based on the responses they elicit. We used 3 different chirps occurring at 2 different phases for a total of 6 stimuli. When comparing the discriminability between 2 sets of responses, a given set of responses included either the responses to a single chirp at a single phase or included the responses to that chirps regardless of the phase at which it occurred.

the responses of 17 cells are pooled. This result does not mean, however, that the population response would allow the decoder to discriminate between chirps if the phase was not fixed. Under natural circumstances, the phase would not be fixed so we repeated our analysis with chirp stimuli that happened at two different phases. Discrimination performance in this case was reduced to near chance levels (i.e., near 50%). These results show that, whereas the structure of the population response allows the discrimination of different AMs, it does not allow the discrimination of different small chirps.

Chirp discrimination: big chirps can be accurately discriminated

The same analysis carried out for big chirps leads to a very different conclusion. The examples of the responses of four I-cells to three big chirps show that differences in the chirps are correlated with differences in the responses (Fig. 5*A*). Notice, for example, that the first cell (*top rows*) has a longer increase in its firing rate after chirp *Y* (*middle*) than chirp *X* (*left*), presumably because chirp *Y* is longer. We used the same analysis as we did for small chirps to determine the discriminability of big chirps. The results confirm that big chirps can easily be discriminated by pooling the responses from seven or eight I-cells (Fig. 5*B*). E-cells respond to big chirps by ceasing their baseline discharge, and the duration of this pause in firing permits the discrimination of different length big chirps (Sup-

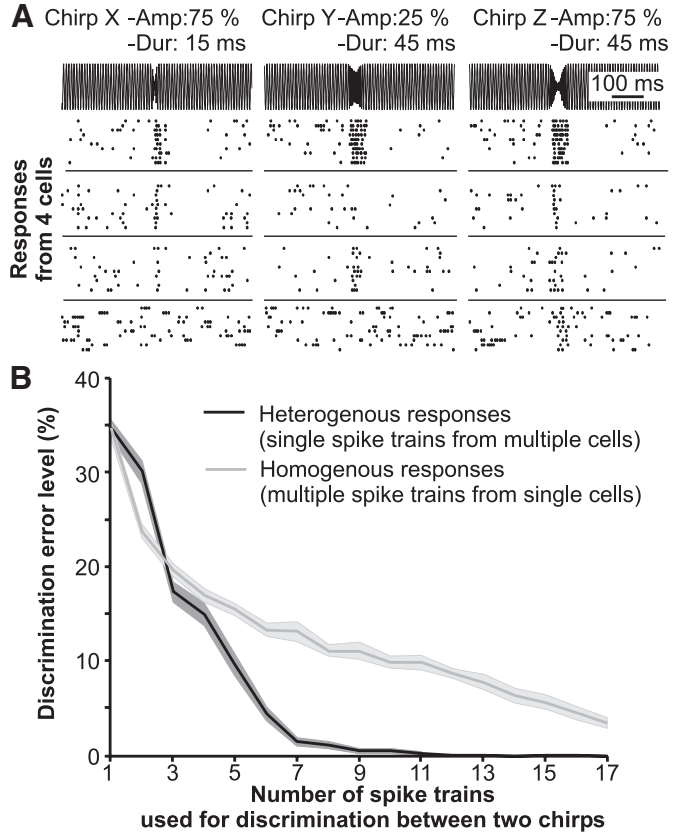

FIG. 5. Discrimination of big chirps by I-cells. *A*: neural responses. We show 3 of the 9 chirps used during the experiment (top traces) followed by raster plots of the responses of 4 cells to several repetitions of the stimulus. These cells were chosen to show the variability in the responses to the chirps within individual pyramidal cells and the much larger variation across cells. We describe the shape of the chirps by their duration (labeled "Dur") and the magnitude of their amplitude decrease (labeled "Amp"). *B*: mean discriminability (±SE; $n = 36$ chirp pairs) of responses to different chirps. In our regular analysis, the different responses combined come from different neurons (heterogeneous response, black line), thus assessing the discriminability of the actual population's response. We repeated the analysis combining several responses from the same neuron, thus assessing the discriminability of the responses if the population was homogeneous (gray line).

plementary Fig. S5). However, differences in the amplitude of the big chirps are not well encoded by E-cells. Although we cannot rule out the possibility that E-cells contribute to the discrimination of big chirps of different duration, I-cells are necessary to discriminate between big chirps of different amplitude and sufficient to allow for accurate discrimination of big chirps of different duration. We therefore focus on the role of I-cells in big chirp discrimination.

Big chirp discrimination and neural heterogeneity

The raster plot in Fig. 5*A* shows that I-cell responses to big chirps vary from cell to cell. This variation reflects differences in the response properties of individual I-cells. For example, the responses of some I-cells are clearly different when the chirps vary in duration (e.g., 1st cell on *top*), whereas other cells will be more strongly affected by the amplitude of the chirp (e.g., 2nd cell from the *top*). This heterogeneity in the population of I-cells could have a functional impact on the coding capacity of the population. More specifically, the heterogeneity could have an impact on the efficiency of coding and thus influence the discrimination accuracy of our putative midbrain decoder. The alternate hypothesis is that the heterogeneity does not improve coding efficiency and thus that a homogeneous population of cells, with the same average response properties, would perform as well. To mimic a homogeneous population of cells we created population responses that combine several responses from the same I-cell. These homogeneous population responses lead to more discrimination errors (Fig. 5*B*).

This analysis based on a measure of spike train distances shows that big chirps can be perfectly discriminated by small populations of I-cells as long as they have heterogeneous response properties. The analysis depends on an arbitrary choice of the temporal resolution with which we evaluate firing rate—the α function width (see METHODS). A width much larger that the mean interspike interval [ISI; mean ISI = 25.5 ± 9.8 (SE) ms] is equivalent to a decoder that evaluates the spike count or mean firing rate of the I-cell's response to the big chirp. At the other extreme, a width much less than the mean ISI is sensitive to the precise timing of the big chirp–evoked spikes and therefore requires a downstream coincidence detector (Larson et al. 2009; Machens et al. 2003). A heterogeneous population of 10–15 I-cells achieves the most reliable discrimination when the temporal resolution is 5–10 ms (Fig. 6*A*). The fact that the mean I-cell ISI evoked by big chirps (mean = 25.5 ± 9.8 ms) is more than two times larger than the optimal temporal resolution suggests that the temporal position of spikes influences the discrimination performance. These results have very specific implications about the characteristics of the decoding circuits (see DISCUSSION) and suggest that some information about the shape of the big chirp stimulus is encoded in the detailed structure of the spike train. We confirmed that spike train structure carries information that could be used for efficient discrimination of big chirps by repeating our analysis after shuffling the temporal position of spikes within each chirp response (Fig. 6*B*). These shuffled responses have the same spike count but altered temporal structures. This operation largely impaired discrimination performance showing that the temporal structures of these responses do potentially carry a significant amount of information about the details of the big chirp's time course.

Heterogeneity improves discrimination when spike count is the main aspect of the response influencing the result (i.e., $\tau >$ 50 ms in Fig. 6), indicating that different big chirps evoke different mean spike counts across the I-cell population. Heterogeneity also improves discrimination when $\tau < 20$ ms (Fig. 6), thus preserving the fine temporal structure of the ISI sequence; heterogeneity in the spike train structure could therefore contribute to better performance of the heterogeneous population response independent of the heterogeneity in spike rate. To assess the influence of the heterogeneity of spike train structure independently of spike rate, we compare (Fig. 7) the spike train distances to the responses correlations (mean subtracted). The correlation between two responses will be determined only by the temporal structure of the spike train as long as the means are subtracted. In this analysis, we compare the responses to two chirps that are relatively similar and thus that are the hardest to discriminate from one another.

In Fig. 7*A,* we show several responses of the same cell to these two chirps displayed as firing rates. Visual inspection of these examples show that two responses to the same chirp are

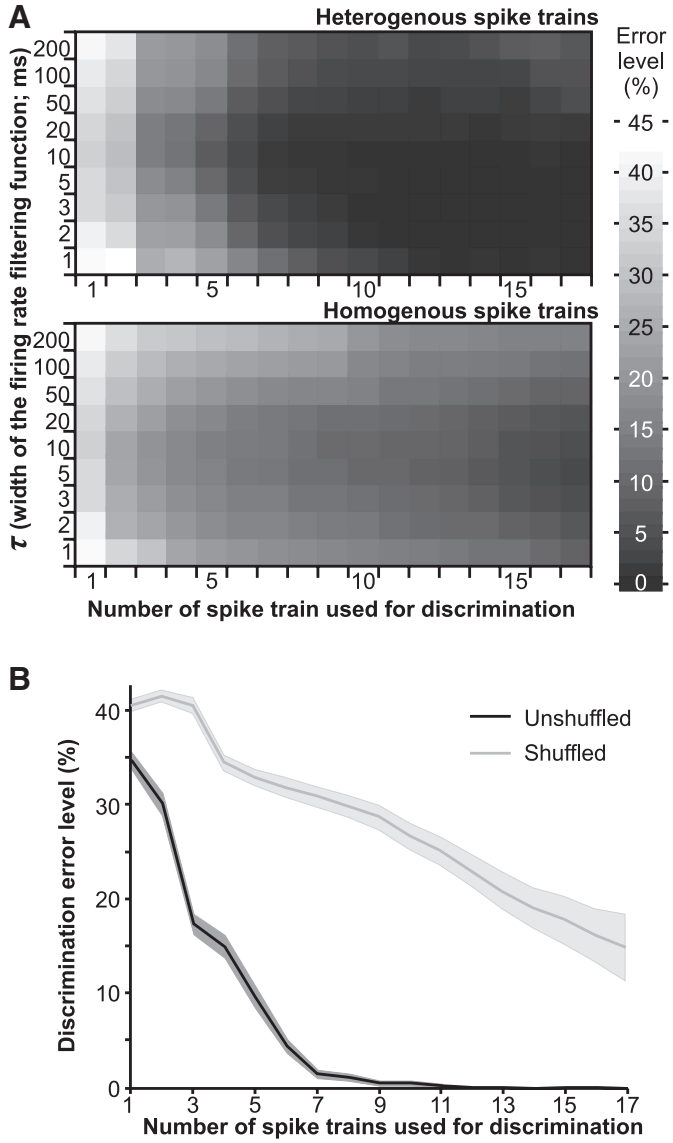

FIG. 6. Spike train structure and chirp discrimination. *A*: temporal resolution of cell response and chirp discrimination. The only free parameter in our analysis is the width of the α function used to convolve with the spike trains. Here we varied the width (i.e., τ) of the function to evaluate the importance of the temporal resolution with which spike trains are compared. The mean discrimination error levels (across 36 chirp pairs) are shown as a gray gradient. *B*: shuffled spike trains and chirp discrimination. The analysis presented in Fig. 5*B* was repeated after shuffling the temporal position of spikes within each response to big chirps. The difference in discrimination accuracy between shuffled (gray) and unshuffled data shows the importance of spike train structure to allow optimal chirp discrimination.

as different from each other as two responses to different chirps. This is quantified in Fig. 7*E* (*left*), where we show the distributions of spike train distances between two responses to the same chirp (gray shading) or between responses to different chirps (black line). The cell's responses to the same chirp are as distant from each other as from responses to a different chirp. The same conclusion prevails for correlations (Fig. 7*E*, *right*): the cell's responses to the same chirp are as correlated as its responses to the different chirp. The total overlap between these distributions (both distances and correlations) indicate that the discrimination performance based on a single response would be near chance level.

When seven responses from the same cell are combined, the variability is reduced (Fig. 7*B*). Although the population responses to different chirps clearly differ, variability in the population responses remains. This is visible in Fig. 7*F* by the fact that the same-chirp distance histogram and different-chirp histogram have different means but are relatively broad. The breadth of the histograms causes them to overlap, and this overlap corresponds to the relatively poor discrimination performance of homogenous spike trains (Figs. 5 and 6); the separation evident here translates into a discrimination error of 24%.

The correlation histograms (Fig. 7*F, right*) illustrate two points. First, the correlations between different population responses to the same chirp vary greatly, and, although the mean is positive, there are cases where responses are negatively correlated. Second, the correlations for responses to the different big chirps vary just as greatly, and, although they are less likely to be very high (near 1), their correlations still overlap extensively with the same-chirp correlations.

Single responses of different I-cells (Fig. 7*C*) also vary extensively, and the resulting population response distance histograms show complete overlap (Fig. 7*G, left*). This is, as might be expected, exactly the same result as that seen for the responses of a single cell (cf. Fig. 7, *A* and *E*). The correlation histogram, however, shows a very striking difference with the situation for a single cell: the mean correlation is now close to 0 and the mode is negative (cf. Fig. 7, *E* and *G*). Different cells tend to give uncorrelated or even slightly negatively correlated responses. In the language of linear algebra, the population response vectors of different I-cells are more likely to be orthogonal than those of the same cell. This observation suggests that the varying temporal structure of big chirps could be represented by a near orthogonal decomposition over a population of I-cells.

When the heterogeneity of the population is taken into account (Fig. 7*D*), the population responses to the same chirp are now very similar and also very different from the population responses to different chirps (cf. Fig. 7, *B* and *D*): in the language of linear algebra, the summation of the responses to one chirp across different I-cells results in convergence to an invariant population vector (response over time) and the invariant vectors differ for different chirps. This is also evident in the narrow distributions (invariance) and the difference in means (different vectors for different chirps) of the response distance histograms (Fig. 7*H, left*; cf. 7*F, left*). The minimal overlap between same-chirp and different-chirp histograms (Fig. 7*H, inset*) corresponds to the excellent estimation performance of heterogonous spike trains (Figs. 5 and 6); the separation evident here translates into a discrimination error of only 8.5%.

The distribution of population response correlations to the same chirp are now narrow and almost always positive. In fact most correlations are close to 1. Again this makes sense from the perspective of an invariant vector—each subset of responses to one chirp sums to nearly the same vector, thus producing a high degree of positive correlation across population responses to that chirp. The correlations across invariant vectors for the two big chirps show less overlap than those generated using the responses of one cell (cf. Fig. 7, *F* and *H, right*). The importance of the heterogeneity in spike train structure can be assessed by comparing the distribution in Fig. 7, *F* and *H* (*right*). We used these distributions to calculate the discrimination performance of a decoder that would rely only on response structure. A homogeneous scenario (Fig. 7*F*)

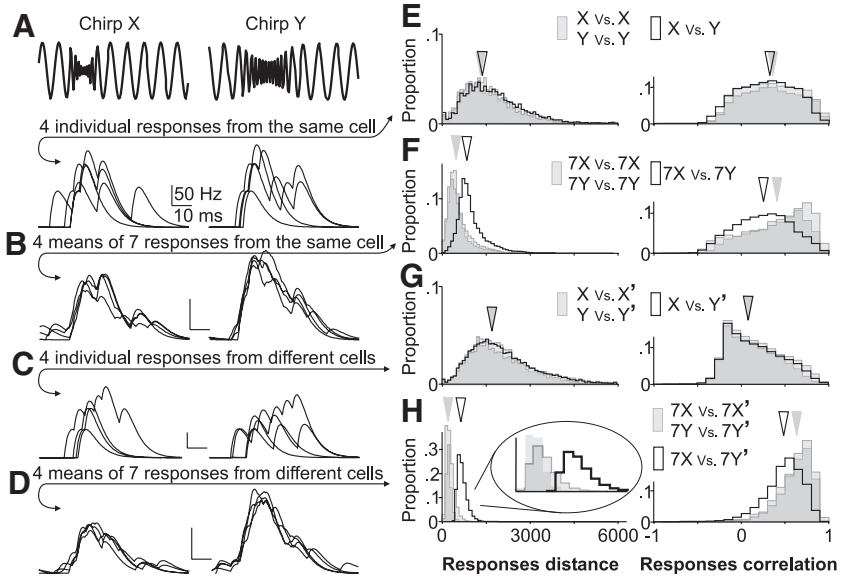

FIG. 7. The heterogeneity of the population leads to an invariant population response. *A–D*: examples of responses to 2 different big chirps (*X*: 15 ms duration, 75% amplitude; *Y*: 30 ms duration, 50% amplitude). The spike trains have been convolved with an α function (τ = 10 ms). *E–H*: quantification of the differences between responses. Difference is quantified either as the spike metric distance as used in Figs. 4–6 (*left*) or as a correlation coefficient (*right*). On each plot, 2 gray histograms represent the difference in responses to a given chirp (either chirp *X* or *Y*). The dark vs. light gray shading represents portions of the histograms that do/do not overlap. The histograms drawn with a black line represent the difference between responses to two different chirps (chirp *X* vs. chirp *Y*, labeled "*X* versus *Y*'). The histograms in the *left plot* of *H* are blown up in the *inset*. The triangles above each histogram indicates its mean. The variability across individual responses from the same cell is shown with an example in *A* and quantified in *E*. Combination of 7 responses from the same cell lead to a reproducible spiking pattern that is different for chirps *X* and *Y* (*B* and *F*). Responses from different cells are on average uncorrelated (*C* and *G*), and combining responses from different cells leads to a highly invariant response vector for a given chirp, easily distinguishable from the responses to a different chirp (*D* and *H*). The apostrophe denotes that the responses come from different cells; e.g., *X* vs. *Y*': responses to chirp *X* and chirp *Y* are from different cells (i.e., heterogeneous scenario).

would lead to 40% discrimination error but only 35% for a heterogeneous scenario; therefore the heterogeneity in response structure also improves the discrimination accuracy.

Temporal coding and neural heterogeneity

The analysis of Figs. 6 and 7 showed that two aspects of the heterogeneity in response properties contribute to improving the discrimination of big chirps: the number of spikes in the responses of different cells and their temporal distribution. A more general way of characterizing the response properties of a cell consists in stimulating it with white noise RAM stimuli and estimating the transfer function of the cell. We therefore recorded the response of these cells to white noise stimuli that have the same overall statistical characteristics as big chirps: a high-frequency beat (AM) modulated by a low-frequency AM envelope (Fig. 1*A*). To replicate the characteristics of chirps, the low-frequency AM envelope contains modulations from 0 to 60 Hz (Supplementary Fig. S2). The *inset* of Fig. 8*A* shows an excerpt of the low-frequency envelope and the response of a pyramidal cell. Comparison of the stimulus-response and response-response coherence (Borst and Theunissen 1999) suggests that these stimuli are encoded in a linear manner (Supplementary Fig. S6). For this reason, we characterize the response to these stimuli by their linear kernels. In a linear system, the kernels are equivalent to the spike triggered averages: the average waveform that triggers a spike. The variability in the kernels of the four cells shown in Fig. 8*A* reflects the differences in response properties of the cells. For example, the kernel with a large initial upstroke would be associated with a cell that is more high-pass. Differences in the amplitude of these kernels can reflect differences in the overall sensitivity and firing rate of the cells.

Differences in response properties will lead each cell to encode different aspects of the stimulus. Using a well-known stimulus reconstruction technique (Borst and Theunissen 1999), we calculated the estimate of the stimulus waveform that can be reconstructed from the response of each cell. Excerpts of these estimates clearly show that different aspects of the stimulus are encoded by different cells (Fig. 8*B, top*). As a consequence, a population of three cells with different response properties will accurately estimate the stimulus waveform (Fig. 8*B, bottom*). To compare this estimate to the way a homogeneous population of cells could estimate the stimulus, we used the same mean kernel (mean across all cells) in the calculation of the stimulus waveform estimate. This homogeneous scenario lead to a less accurate estimate of the stimulus (Fig. 8*B, middle*) compared with combining the responses of the three cells using their individually matched kernels (Fig. 8*B, bottom*).

The difference between the estimate and the actual stimulus can be used to calculate the amount of information that the response carries about the stimulus. When the calculation takes into account the diversity of the kernels of each cell, the population response encodes equally well all AM frequencies present in the stimulus. We replaced the kernel of each cell by the average kernel across cells, thus mimicking a homogeneous population of cells with the same filtering characteristics (Fig. 8*C*). The difference in the information transfer functions in Fig. 8*C* indicates that assuming that the population is homogeneous does not allow us to decode all the information present in the response. Specifically, the decoder that uses the matched kernels extracts more information at high frequencies (>20 Hz; Fig. 8*C*) than the decoder using a mean kernel. This again implies that the heterogeneity of

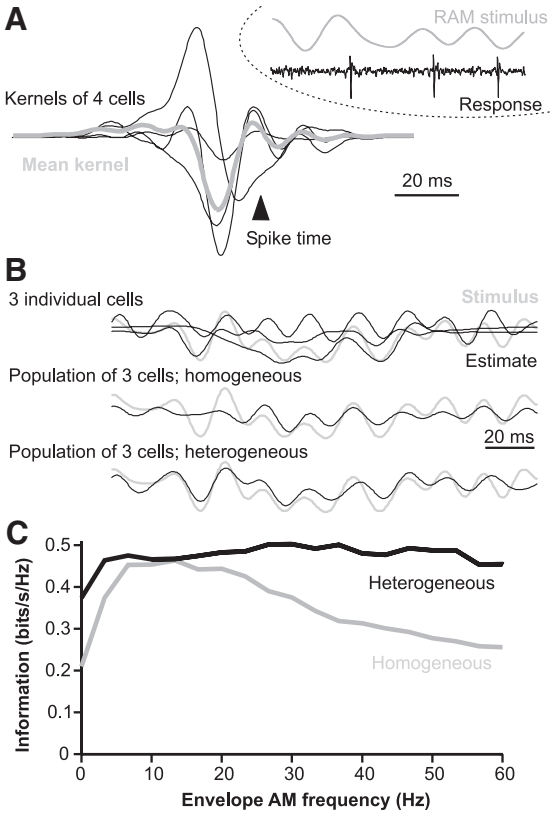

FIG. 8. Temporal coding by I-cells. *A*: filtering characteristics of I-cells determined from the responses to random amplitude modulated stimuli. We delivered stimuli containing the same kind of modulations as big chirps: low-frequency (0–60 Hz) envelope modulations of a high-frequency beat (200 Hz). The random envelope modulations and the responses they elicit (excerpt shown in the *inset*) can be used to calculate the cell's kernel. This kernel characterizes the linear filtering properties of the cell. The kernels from 4 cells are shown here to illustrate the diversity in response properties along with the average kernel ($n = 19$ cells). *B*: estimates of the stimulus based on the cell's responses and their kernel. Convolution of the spike trains with the kernel allows the reconstruction of a stimulus estimate. We show examples of such reconstructions in 3 different scenarios. *Top*: 3 responses from a given cell are combined and convolved with the kernel of that cell. The estimates from individual cells are shown to illustrate how each cell encodes different aspects of the stimulus. We combined 3 responses to base our reconstruction on similar number of spikes as in the *middle* and *bottom* estimates. *Middle*: 3 responses coming from different cells are combined and convolved with the mean kernel across cells. This manipulation mimics a situation where each cell is equivalent, thus averaging their kernel leads to averaging out the noise in the kernel estimate. *Bottom*: 3 responses from different cells are convolved with their respective (i.e., different) kernels. This estimate can benefit fully from the heterogeneity of the population. *C*: information transfer functions. The difference between the stimulus and the estimate can be used to calculate the amount of information about the stimulus carried by the response. Information transfer was calculated as a function of frequency of envelope modulation (Hz) based on combined estimates from 17 cells. The kernel used to calculate the estimate was either the mean kernel across all cells (gray lines) or the individual kernels of each cell (black lines).

responses plays an important role in encoding information about the fine structure of big chirp stimuli.

DISCUSSION

Small chirps versus big chirps

As might be expected (Marler 2004), electric fish use different communication signals during agonistic versus courtship interactions, and these signals cause opposite effects on the synchronization of the electroreceptors (Benda et al. 2006). We showed that two disjoint target subpopulations of pyramidal cells decode the evoked electroreceptor synchronization (E-cells) or de-synchronization (I-cells). In accordance with Barlow's dictum, this sparsification of the neural code is an efficient coding strategy inasmuch as target TS circuits (Carr and Maler 1986) selective for E and I input (Metzner and Heiligenberg 1991) could, in principle, readily differentiate small and big chirps.

We also showed that small and big chirps are encoded using entirely different coding strategies. Small chirps are encoded by a small number of superficial E-cells of the lateral ELL map (~150 cells in one ELL; Maler 2009a) via spike bursts. The LS E-cell bursts sensitively detect small chirps but cannot effectively discriminate among them. It requires only ~10 such cells to detect the small chirps used in our experiments. Presumably the larger number of available E-cells would permit the fish to detect the weaker signals of more distant males.

In contrast, big chirps are encoded by firing rate modulations of numerous I-cells across all the ELL maps (~2,500 cells in one ELL; Maler 2009a); the firing rates of only a small subset (~10 cells) can provide an accurate estimate of big chirp quality and discriminate even small differences among them. Under natural conditions the discrimination task might well be much more difficult for two reasons. First, the fish might be at greater distances and therefore produce far weaker AMs. Second, the big chirps will be superimposed on beats with a large range of frequencies, and it is possible that for some beat frequencies big chirps discrimination is harder to achieve. We hypothesize that the very large number of available I-cells will permit a female to discriminate a wide range of big chirp shapes even under a wider range of natural conditions.

Courtship signals usually transmit information about the fitness of the emitter (Andersson 1994; Zahavi 1975). Big chirps are mostly produced by a male to court females and are emitted at slow rates, typically a few per minute (Bastian et al. 2001; Hupé and Lewis 2008). Because big chirps involve doubling the EOD frequency for tens of milliseconds, they might be costly to produce, suggesting that their duration and magnitude (i.e., the increase in EOD frequency) can signal the fitness of the fish or its readiness to spawn (Dulka et al. 1995). It is therefore crucial for the sensory system to preserve the information contained in the shape of big chirps so that downstream circuitry can process it further. We argue that the ELL performs well in this respect by providing an accurate linear description of the temporal features of big chirps.

Small chirps are encoded by synchronous bursting in superficial LS E-cells (Marsat et al. 2009). We showed that this response allows the accurate detection of the chirp but provides limited information about its characteristics. This is mostly because of the fact that the shape of a small chirp's signal is largely determined by the phase of the beat at which it occurs (Benda et al. 2005; Marsat et al. 2009; Zupanc and Maler 1993) and thus is unlikely to carry information about the quality of the chirp. It does not mean that bursts cannot encode the shape of the events they signal. Indeed, it has been shown in vitro that the ISIs within bursts carry information about the intensity of the stimulus (Oswald et al. 2007). Our experiments also show that the burst response allows, in principle, the discrimination of signals with different modulation shapes, although it is not

as accurate as for the responses to big chirps. We suggest that bursts are an efficient neural code for signaling the occurrence of specific events (i.e., feature detectors) but that their stereotyped nature limits their capacity to convey detailed information about the shape of these events. This argument is supported by the fact that the burst response to small chirps does not permit a discrimination of EOD amplitude shape as accurately as does the graded response of I-cells to big chirps (cf. Figs. 4*B,* fixed phase, and 5*B,* heterogeneous). The complex relationship between the characteristics of small chirps as they are emitted and the shape of the AM they produce suggests that the quality of this communication signal could be carried by another aspect of the signal. The rate of emission of small chirps is variable and can be as high as a few chirps per second during close range interactions (Hupé and Lewis 2008). Furthermore, the emission rate depends on the hormonal status of the fish (Dulka and Maler 1994; Dunlap et al. 1998); it is therefore plausible that the quality of an aggressive display is more related to small chirp rate rather than chirp shape. We argue that the nature of these two neural codes perfectly fits the tasks the system has to achieve by transforming the signals into a format that allows downstream neural networks to readily access relevant information. They therefore constitute, in Barlow's sense, efficient codes.

Signal discrimination and decoding of population responses

The spike train metric developed by Victor and Purpura (1996, 1997) and its variant developed by van Rossum (2001) can be used to estimate how well two stimuli can be discriminated based on the responses they elicit and is related to the amount of information the spike trains carry about the stimuli. These methods have been applied to the study of single neuron responses in many systems (Machens et al. 2003; Narayan et al. 2007; Ronacher et al. 2008; Samonds and Bonds 2004; Victor 2005). For example Machens et al. (2003) asked how many seconds of the spike trains elicited by a grasshopper song are needed to discriminate between two individuals. We extended the van Rossum (2001) technique to populations of neurons and examined the discrimination performance as a function of cell number. As expected, there was a steep improvement in accuracy when the responses of many cells are summed. Discrimination accuracy could, in principle, be improved if different weights were applied to the responses of different cells; however, this procedure precludes assuming that the population of cells is homogenous and thus all their responses equivalent.

The van Rossum method is particularly relevant here because it can be readily implemented by biologically plausible networks (Larson et al. 2009). In particular, it permits an estimation of the temporal resolution of an optimal decoding circuit. In vivo studies in several systems (Desbordes et al. 2008; Machens et al. 2003; Narayan et al. 2006; Wohlgemuth and Ronacher 2007) have found optimal decoding with a 5–10 ms filter width, a value identical to that reported here. This resolution is not only optimal from the point of view of the decoder but, in at least some cases, was also found to be the typical temporal precision of encoding populations of neurons. For example, a study of the visual system (Desbordes et al. 2008) showed that a 10 ms temporal precision characterized the population code entering the cortex. For ELL I-cell output, this time scale implies a decoding mechanism in which the structure of the spike train is important but that requires spike timing precision of only a few milliseconds. Remarkably, the duration of pyramidal cell evoked excitatory postsynaptic potentials (EPSPs) in TS neurons seems to be <10 ms in duration (see Fig. 9*A* in Fortune and Rose 2000). Chirp-sensitive neurons have been found in the TS (K. Vonderschen and M. J. Chacron, personal communication), and it may therefore be possible to determine whether a van Rossum type decoder with a 5–10 ms filter is operating in TS to process big chirps.

Heterogeneity and population coding efficiency

Population coding is an ubiquitous feature of nervous systems, but it is inevitably corrupted by the noisy spiking responses of its constituent neurons (Pouget et al. 2000). The simplest readout of a noisy population code would be for the decoding network to remove noise by simply averaging the neural response over subsets of the input population. Initial studies assumed that noise removal capacity will be reduced when the population has correlated noise activity (Sompolinsky et al. 2001). In the ELL, correlated noise in the responses is observed only among neurons with overlapping receptive fields (Chacron and Bastian 2008), which means that many of the neurons responding to chirps will not show correlated noise. Furthermore, these authors also showed that noise correlations are reduced in the presence of communication signals because of the activation of global feedback inputs. Our experiments were single cell recordings, thus preventing us from directly quantifying noise correlations of the population response and its impact on information coding. However, considering the limited noise correlations observed (Chacron and Bastian 2008), we suggest that they will not be an important limit to noise removal from the population response. Furthermore, recent theoretical studies have shown that, if the population of neurons is heterogeneous, as is the case for ELL I-cells, correlated noise does not greatly limit information transmission (Osborne et al. 2008; Shamir and Sompolinsky 2006). Nevertheless, we cannot exclude the possibility that correlated noise among pyramidal cell responses reduces the amount of information transmitted about chirps, and our measures therefore represent an upper bound of the actual performance of the system.

Heterogeneity in a population of neurons can also potentially improve coding efficiency by causing the cells to encode differently the detailed time course of the stimulus. We showed that I-cell heterogeneity acts to de-correlate the representation of the signal, which amounts to encoding the stimulus in a less redundant way. ELL pyramidal cells are organized into columns (3 E- and I-cells per column; Maler 2009a) and three maps (Maler 2009a,b). All I-cells have generally similar tuning properties (e.g., they are mostly low-pass; Krahe et al. 2008; Mehaffey et al. 2008), and all respond to big chirps, but they differ in a variety of manners (e.g., channel composition, size of apical dendritic tree, spontaneous firing rate; Maler 2009a,b). Although the detailed biophysical heterogeneity of I-cells needs further characterization, it undoubtedly underlies the diversity of I-cell responses to the same big chirp, and thus we hypothesize, enhances their big chirp coding efficiency.

Our analysis shows that a certain amount of information about the shape of big chirps is encoded in the average spike count of the population response (Fig. 6*A*; $\tau > 50$ ms). Additional information is carried by the temporal structure of

the response (Fig. 6*A* for $\tau < 20$ ms; Figs. 7 and 8). We presented several lines of evidence in favor of this hypothesis in particular by showing that temporal smoothing of a spike train (Fig. 6*A*; $\tau > 50$) or shuffling of spike times (Fig. 6*B*) can reduce the discrimination accuracy. This is consistent with numerous findings stressing the importance of the temporal structure of spike trains for information coding; in particular, it was recently directly shown that a population spike count code would be insufficient to account for the accuracy of a visual discrimination task (Jacobs et al. 2009). Our results also point out that the heterogeneity of both these aspects of the response—spike count and temporal response structure—improves the quality of encoding. Because part of the information is encoded in the temporal structure of the spike trains, a decoder would have to exploit this aspect of the response; the details of how such a decoder might work have not been explored. The TS neurons responsive to big chirps (K. Vonderschen and M. J. Chacron, personal communication) might therefore offer an opportunity to investigate such putative temporal pattern decoders.

The role of heterogeneity in improving coding efficiency has been the focus of recent studies in mammalian cortex and midbrain. In particular, it has been shown that the heterogeneity in firing patterns of MT neurons in the visual cortex of primates leads to an increase in information coding (Osborne et al. 2008). Another study showed that heterogeneity of the population response of neurons in the inferior colliculus of mammals permits the discrimination of different vocalizations (Holmstrom et al. 2010). Sensory coding is often referred to as sparse in higher brain areas because only a few neurons respond to a given feature of the sensory signal so that these features are not redundantly encoded in a large population of neurons (Olshausen and Field 2004). On the other hand, coding at the periphery is typically very redundant (Puchalla et al. 2005). To our knowledge, this study is the first demonstration of the importance of heterogeneity at the lowest level of the CNS (the ELL receives inputs directly from sensory electroreceptors). We describe here the initial step in the CNS toward the sparsification of sensory coding, and our results indicate that neuronal heterogeneity is an important contributor to this process.

In summary, our results show two levels of sparsification. At a coarse level, different communication signals are encoded by separate populations of pyramidal cells, and these populations use entirely different neural codes. We suggest that the differences in neural codes used in each case reflect whether the signals need to be merely detected (agonistic signals, E-cell burst code) or discriminated as well as detected (courtship signals, I-cell time-dependent rate code). On a finer level, the heterogeneity of I-cell responses to courtship signals can improve discrimination in two ways. First, it allows for effective averaging across a population of neurons that are, on average, not highly correlated in their responses. Second, the heterogeneity of responses might also permit the decoding circuits to use I-cell spike temporal patterning more effectively to further improve big chirp discrimination and therefore improve mate choice in these electric fish.

ACKNOWLEDGMENTS

We thank Dr. Rüdiger Krahe for providing recordings of big chirps; Dr. Jan Benda, W. Ellis, and Dr. André Longtin for technical help and useful discussions; B. Elliott for proofreading; and the anonymous reviewers for useful comments.

GRANTS

This work was supported by grants from Canadian Institutes of Health Research to G. Marsat and L. Maler.

DISCLOSURES

No conflicts of interest, financial or otherwise, are declared by the author(s).

REFERENCES

Aertsen AMHJ, Gerstein GL, Habib MK, Palm G. Dynamics of neuronal firing correlation—modulation of effective connectivity. *J Neurophysiol* 61: 900–917, 1989.

Andersson MB. *Sexual Selection*. Princeton, NJ: Princeton University Press, 1994.

Barlow HB. Possible principles underlying the transformation of sensory messages. In: *Sensory Communication*, edited by Rosenblith WA. Cambridge, MA: MIT Press, 1961, p. 217–234.

Bastian J, Nguyenkim J. Dendritic modulation of burst-like firing in sensory neurons. *J Neurophysiol* 85: 10–22, 2001.

Bastian J, Schniederjan S, Nguyenkim J. Arginine vasotocin modulates a sexually dimorphic communication behavior in the weakly electric fish *Apteronotus leptorhynchus*. *J Exp Biol* 204: 1909–1924, 2001.

Bell AJ, Sejnowski TJ. An information-maximization approach to blind separation and blind deconvolution. *Neural Comput* 7: 1129–1159, 1995.

Benda J, Longtin A, Maler L. Spike-frequency adaptation separates transient communication signals from background oscillations. *J Neurosci* 25: 2312–2321, 2005.

Benda J, Longtin A, Maler L. A synchronization-desynchronization code for natural communication signals. *Neuron* 52: 347–358, 2006.

Berman N, Maler L. Neural architecture of the electrosensory lateral line lobe: adaptations for coincidence detection, a sensory searchlight and frequency-dependent adaptive filtering. *J Exp Biol* 202: 1243–1253, 1999.

Borst A, Theunissen FE. Information theory and neural coding. *Nat Neurosci* 2: 947–957, 1999.

Carr CE, Maler L. Electroreception in gymnotiform fish: central anatomy and physiology. In: *Electroreception*, edited by Bullock TH, Heiligenberg W. New York: Wiley, 1986, p. 319–374.

Carr CE, Maler L, Sas E. Peripheral organization and central projections of the electrosensory nerves in gymnotiform fish. *J Comp Neurol* 211: 139–153, 1982.

Chacron MJ, Bastian J. Population coding by electrosensory neurons. *J Neurophysiol* 99: 1825–1835, 2008.

Chechik G, Anderson MJ, Bar-Yosef O, Young ED, Tishby N, Nelken I. Reduction of information redundancy in the ascending auditory pathway. *Neuron* 51: 359–368, 2006.

Chelaru MI, Dragoi V. Efficient coding in heterogeneous neuronal populations. *Proc Natl Acad Sci USA* 105: 16344–16349, 2008.

Clague H, Theunissen F, Miller JP. Effects of adaptation on neural coding by primary sensory interneurons in the cricket cercal system. *J Neurophysiol* 77: 207–220, 1997.

Desbordes G, Jin J, Weng C, Lesica NA, Stanley GB, Alonso J-M. Timing precision in population coding of natural scenes in the early visual system. *PLoS Biol* 6: , 2008.

Dulka JG, Maler L. Testosterone modulates female chirping behavior in the weakly electric fish, *Apteronotus leptorhynchus*. *J Comp Physiol A* 174: 331–343, 1994.

Dulka JG, Maler L, Ellis W. Androgen-induced changes in electrocommunicatory behavior are correlated with changes in substance P-like immunoreactivity in the brain of the electric fish *Apteronotus leptorhynchus*. *J Neurosci* 15: 1879–1890, 1995.

Dunlap KD, Larkins-Ford J. Diversity in the structure of electrocommunication signals within a genus of electric fish, *Apteronotus*. *J Comp Physiol A* 189: 153–161, 2003.

Dunlap KD, Thomas P, Zakon HH. Diversity of sexual dimorphism in electrocommunication signals and its androgen regulation in a genus of electric fish, *Apteronotus*. *J Comp Physiol A* 183: 77–86, 1998.

Engler G, Fogarty CM, Banks JR, Zupanc GK. Spontaneous modulations of the electric organ discharge in the weakly electric fish, *Apteronotus*

leptorhynchus: a biophysical and behavioral analysis. *J Comp Physiol A* 186: 645–660, 2000.

Fortune ES, Rose GJ. Short-term synaptic plasticity contributes to the temporal filtering of electrosensory information. *J Neurosci* 20: 7122–7130, 2000.

Frank K, Becker MC. Microelectrodes for recording and stimulation. In: *Physical Techniques in Biological Research*, edited by Nastuk WL. New York: Academic Press, 1964, p. 23–84.

Hagedorn M, Heiligenberg W. Court and spark—electric signals in the courtship and mating of gymnotoid fish. *Anim Behav* 33: 254–265, 1985.

Heiligenberg W, Dye J. Labeling of electroreceptive afferents in a Gymnotoid fish by intracellular injection of HRP—the mystery of multiple maps. *J Comp Physiol A* 148: 287–296, 1982.

Holmstrom LA, Eeuwes LB, Roberts PD, Portfors CV. Efficient encoding of vocalizations in the auditory midbrain. *J Neurosci* 30: 802–819, 2010.

Hopkins CD. Sex differences in electric signaling in an electric fish. *Science* 176: 1035–1037, 1972.

Hupé GJ, Lewis JE. Electrocommunication signals in free swimming brown ghost knifefish, *Apteronotus leptorhynchus*. *J Exp Biol* 211: 1657–1667, 2008.

Jacobs AL, Fridman G, Douglas RM, Alam NM, Latham PE, Prusky GT, Nirenberg S. Ruling out and ruling in neural codes. *Proc Natl Acad Sci USA* 106: 5936–5941, 2009.

Kelly M, Babineau D, Longtin A, Lewis JE. Electric field interactions in pair of electric fish: modeling and mimicking naturalistic inputs. *Biol Cybern* 98: 479–490, 2008.

Krahe R, Bastian J, Chacron MJ. Temporal processing across multiple topographic maps in the electrosensory system. *J Neurophysiol* 100: 852–867, 2008.

Larson E, Billimoria CP, Sen K. A biologically plausible computational model for auditory object recognition. *J Neurophysiol* 101: 323–331, 2009.

Machens CK, Schutze H, Franz A, Kolesnikova O, Stemmler MB, Ronacher B, Herz AV. Single auditory neurons rapidly discriminate conspecific communication signals. *Nat Neurosci* 6: 341–342, 2003.

Maler L. Neural strategies for optimal processing of sensory signals. *Prog Brain Res* 165: 135–154, 2007.

Maler L. The posterior lateral line lobe of certain gymnotoid fish: quantitative light microscopy. *J Comp Neurol* 183: 323–363, 1979.

Maler L. Receptive field organization across multiple electrosensory maps. I. Columnar organization and estimation of receptive field size. *J Comp Neurol* 516: 376–393, 2009a.

Maler L. Receptive field organization across multiple electrosensory maps. II. Computational analysis of the effects of receptive field size on prey localization. *J Comp Neurol* 516: 394–422, 2009b.

Maler L, Sas E, Johnston S, Ellis W. An atlas of the brain of the electric fish Apteronotus leptorhynchus. *J Chem Neuroanat* 4: 1–38, 1991.

Marler P. Bird calls: their potential for behavioral neurobiology. *Ann NY Acad Sci* 1016: 31–44, 2004.

Marsat G, Proville RD, Maler L. Transient signals trigger synchronous bursts in an identified population of neurons. *J Neurophysiol* 102: 714–723, 2009.

Mehaffey WH, Maler L, Turner RW. Intrinsic frequency tuning in ELL pyramidal cells varies across electrosensory maps. *J Neurophysiol* 99: 2641–2655, 2008.

Metzner W, Heiligenberg W. The coding of signals in the electric communication of the gymnotiform fish Eigenmannia: from electroreceptors to neurons in the torus semicircularis of the midbrain. *J Comp Physiol A* 169: 135–150, 1991.

Metzner W, Juranek J. A sensory brain map for each behavior? *Proc Natl Acad Sci USA* 94: 14798–14803, 1997.

Middleton JW, Longtin A, Benda J, Maler L. The cellular basis for parallel neural transmission of a high-frequency stimulus and its low-frequency envelope. *Proc Natl Acad Sci USA* 103: 14596–14601, 2006.

Miller EK, Nieder A, Freedman DJ, Wallis JD. Neural correlates of categories and concepts. *Curr Opin Neurobiol* 13: 198–203, 2003.

Narayan R, Best V, Ozmeral E, McClaine E, Dent M, Shinn-Cunningham B, Sen K. Cortical interference effects in the cocktail party problem. *Nat Neurosci* 10: 1601–1607, 2007.

Narayan R, Grana G, Sen K. Distinct time scales in cortical discrimination of natural sounds in songbirds. *J Neurophysiol* 96: 252–258, 2006.

Nelson ME, Xu Z, Payne JR. Characterization and modeling of P-type electrosensory afferent responses to amplitude modulations in a wave-type electric fish. *J Comp Physiol A* 181: 532–544, 1997.

Olshausen BA, Field DJ. Sparse coding of sensory inputs. *Curr Opin Neurobiol* 14: 481–487, 2004.

Osborne LC, Palmer SE, Lisberger SG, Bialek W. The neural basis for combinatorial coding in a cortical population response. *J Neurosci* 28: 13522–13531, 2008.

Oswald AM, Doiron B, Maler L. Interval coding. I. Burst interspike intervals as indicators of stimulus intensity. *J Neurophysiol* 97: 2731–2743, 2007.

Pouget A, Dayan P, Zemel R. Information processing with population codes. *Nat Rev Neurosci* 1: 125–132, 2000.

Press WH, Flanney BP, Teukolsky SA, Vetterling WT. *Numerical Recipes in C: The Art of Scientific Computing*. Cambridge, MA: Cambridge University Press, 1992.

Puchalla JL, Schneidman E, Harris RA, Berry MJ. Redundancy in the population code of the retina. *Neuron* 46: 493–504, 2005.

Ronacher B, Wohlgemuth S, Vogel A, Krahe R. Discrimination of acoustic communication signals by grasshoppers (*Chorthippus biguttulus*): temporal resolution, temporal integration, and the impact of intrinsic noise. *J Comp Psychol* 122: 252–263, 2008.

Samonds JM, Bonds AB. From another angle: differences in cortical coding between fine and coarse discrimination of orientation. *J Neurophysiol* 91: 1193–1202, 2004.

Saunders J, Bastian J. The physiology and morphology of 2 types of electrosensory neurons in the weakly electric fish *Apteronotus leptorhynchus*. *J Comp Physiol* 154: 199–209, 1984.

Shamir M, Sompolinsky H. Implications of neuronal diversity on population coding. *Neural Comput* 18: 1951–1986, 2006.

Sompolinsky H, Yoon H, Kang K, Shamir M. Population coding in neuronal systems with correlated noise. *Phys Rev E* 64: 051904, 2001.

Theunissen F, Roddey JC, Stufflebeam S, Clague H, Miller JP. Information theoretic analysis of dynamical encoding by four identified primary sensory interneurons in the cricket cercal system. *J Neurophysiol* 75: 1345–1364, 1996.

Turner CR, Derylo M, de Santana CD, Alves-Gomes JA, Smith GT. Phylogenetic comparative analysis of electric communication signals in ghost knifefishes (Gymnotiformes: Apteronotidae). *J Exp Biol* 210: 4104–4122, 2007.

Turner RW, Lemon N, Doiron B, Rashid AJ, Morales E, Longtin A, Maler L, Dunn RJ. Oscillatory burst discharge generated through conditional backpropagation of dendritic spikes. *J Physiol Paris* 96: 517–530, 2002.

van Rossum MC. A novel spike distance. *Neural Comput* 13: 751–763, 2001.

Victor JD. Spike train metrics. *Curr Opin Neurobiol* 15: 585–592, 2005.

Victor JD, Purpura KP. Metric-space analysis of spike trains: theory, algorithms and application. *Network Comp Neural* 8: 127–164, 1997.

Victor JD, Purpura KP. Nature and precision of temporal coding in visual cortex: a metric-space analysis. *J Neurophysiol* 76: 1310–1326, 1996.

Wohlgemuth S, Ronacher B. Auditory discrimination of amplitude modulations based on metric distances of spike trains. *J Neurophysiol* 97: 3082–3092, 2007.

Zahavi A. Mate selection-a selection for a handicap. *J Theor Biol* 53: 205–214, 1975.

Zakon HH, Dunlap KD. Sex steroids and communication signals in electric fish: A tale of two species. *Brain Behav Evolut* 54: 61–69, 1999.

Zupanc GKH, Maler L. Evoked chirping in the weakly electric fish *Apteronotus leptorhynchus*—a quantitative biophysical analysis. *Can J Zool* 71: 2301–2310, 1993.